

Antibody Markers for Studying Neurodegeneration in the *Nothobranchius* Central Nervous System

T. Genade* and D.M. Lang

Human Biology, Faculty of Health Sciences, University of Cape Town, Private Bag X3, Observatory, 7935, South Africa

Abstract

Fish of the genus *Nothobranchius* have a naturally short lifespan in which they develop several neurological biomarkers of aging. This short lifespan (several months compared to several years in mice and zebrafish) make these fish a promising alternative in aging research. Resveratrol dosing retarded the development of the neurological biomarkers of aging identified in *N. furzeri*. Resveratrol's method of action was not determined due to the lack of cell-type specific markers of degenerative processes. Further research of the *Nothobranchius* CNS and its degeneration is hampered by the lack of cell-type specific antibodies and other cellular markers of degenerative processes.

In this article the authors present a molecular toolbox of five antibodies and a lectin which can be used to study the *Nothobranchius* central nervous system and its degeneration. These antibodies were tested against western blots of rat, zebrafish and *Nothobranchius guentheri* brain homogenates as well as frozen sections. Antibodies shown to reliably bind with *N. guentheri* proteins were: SMI31 which labeled axons and dendrites; mouse anti-human GFAP and rabbit anti-cow GFAP which labeled astroglia; mouse anti-rat tenascin-R which labeled oligodendrocytes; and E587 anti-goldfish L1 which labeled neuronal and astrocytic cell bodies and processes. The BS-I isolectin B4 labeled microglia in the optic nerve and retina.

This toolbox will enable researchers to study the aging brain of *Nothobranchius* as well as its normal development at a cellular level.

Keywords: GFAP; GS-isolectin; L1; Microglia; Neurodegeneration; *Nothobranchius*; SMI31; tenascin-R

Abbreviations: CNS- Central Nervous System; DAB- 3,3'-Diaminobenzidine; GFAP- Glial Fibrillary Acid Protein; IHC- Immunohistochemistry; Lsg- Lower stratum griseum intermediale; NFT-Neuro Fibrillary Tangle; ON- Optic Nerve; OT- Optic Tectum; SAI- Stratum Album Intermediale; SGI- Stratum Griseum Intermediale; SGS- Stratum Griseum Superficiale; SO- Stratum Opticum; SGPV- Stratum griseum periventriculare; SZ- Stratum Zonale; TNR- Tenascin-R; Usgi- Upper stratum griseum intermediale

Introduction

Fish of the genus *Nothobranchius*, Peters, 1844 have a naturally short lifespan in which they develop several neurological biomarkers of aging [1]. Due to its short average lifespan of eight weeks (compared to three to five years for other vertebrate models) *Nothobranchius furzeri* is an excellent model organism for aging research. The aging of *N. furzeri* Jubb, 1971 progressed with an accumulation of lipofuscin and senescence associated β -galactosidase expression [1,2] as well as a decline in operant learning and muscle strength which were correlated with neurodegeneration [2-4]. These age-related phenomena were retarded by resveratrol treatment [3]. Further research of the neuroprotective effect of resveratrol and degeneration of the *Nothobranchius* CNS¹ are hampered by the lack of cell-type specific antibodies and other cellular markers of degenerative processes. Such markers are also needed to render results obtained in *Nothobranchius* comparable to other organisms for the elucidation of general mechanisms of aging and neuroprotection.

For our study frozen sections of *N. guentheri* were prepared on which to test the antibodies and lectin. We focused our research on the visual system as this is well characterized in fish and was the focus of Valenzano et al. [3]. We assembled a toolbox of markers to study the aging of the *Nothobranchius* CNS by testing CNS markers of

development, regeneration and degeneration which have been used on other species. Of ten antibodies tested, the five mentioned below displayed useful reactivity in *N. guentheri*.

The SMI31 antibody recognizes phosphorylated neurofilament protein in neurons, axons, dendrites and neurofibrillary tangles (NFTs) in sections in a diverse array of species. Its accumulation in degenerate neurons is well documented [5,6]. Glial fibrillary acid protein (GFAP), expressed by astroglia, is upregulated following CNS injury and in the process of neurodegeneration [7]. This pathological upregulation is typical of several model organisms making the availability of a GFAP antibody important to *Nothobranchius* aging research.

L1 is a glycoprotein neural recognition molecule of the CAM-immunoglobulin superfamily related to NCAM [8] which has evolved from a family of evolutionary well conserved proteins [9]. It is expressed by astrocytes, oligodendrocytes and growing axons in zebrafish, and is involved in development, regeneration, plasticity and maintaining synaptic contact [8-11]. It has also been implicated in neurodegeneration through the work of Strekova et al. [12].

Tenascin-R (TNR) is a matrix glycoprotein expressed by oligodendrocytes and is implicated in CNS regeneration and axonal path-finding [10,13]. It has been reported to act as a barrier to

*Corresponding author: Dr. T. Genade, Human Biology, Faculty of Health Sciences, University of Cape Town, Private Bag X3, Observatory, 7935, South Africa, Tel: +27214066553; Fax: +27214487226; E-mail: tgenade@gmail.com

Received April 08, 2011; Accepted April 29, 2011; Published May 02, 2011

Citation: Genade T, Lang DM (2011) Antibody Markers for Studying Neurodegeneration in the *Nothobranchius* Central Nervous System. J Cytol Histol 2:120. doi:10.4172/2157-7099.1000120

Copyright: © 2011 Genade T, et al. This is an open-access article distributed under the terms of the Creative Commons Attribution License, which permits unrestricted use, distribution, and reproduction in any medium, provided the original author and source are credited.

microglial migration in tissue culture experiments [14] and plays what is thought to be a neuroprotective role. However, no such microglial repulsion effect was observed in the lizard species *Gallotia galloti* [13]. TNR is associated with lipid rafts where they form a scaffold for signaling proteins such as integrins [15]. Disruption of integrin signaling is linked with impaired neurogenesis [16,17] and inhibition of apoptosis of degenerate neurons [18]. TNR appears to be linked to many facets of CNS development, maintenance and degeneration (as well as regeneration) but is largely unexplored in these regards.

Microglia are involved in CNS inflammation, after insult, and in the course of neurodegeneration [7,19,20]. Kim et al. [21] demonstrated an increase in microglial proliferation in mice in the course of normal aging and after CNS insult, as well as a relative decrease in aging associated proliferation with calorie restriction, using BS-I Isolectin B4. The role of microglia in degeneration is still disputed and it would be useful to know if and how resveratrol and other anti-aging interventions affect them during the course of aging. There is evidence that resveratrol exerts a neuroprotective role in vitro by inhibiting neuroinflammation [20,22]. The availability of a *Nothobranchius* microglial marker would enable us to test this hypothesis in situ using *Nothobranchius*.

Immunohistochemistry studies on sections show that these cellular probes reliably label specific cell types in the *Nothobranchius* CNS. This was supported by western blots which yielded similar banding patterns to other species using the aforementioned antibodies. These results enable research at the cellular level into neurodegeneration and resveratrol induced neuroprotection in *Nothobranchius*.

Materials and Methods

Captive maintenance of *N. guentheri*

N. guentheri were obtained from Mr. O. Schmidt of Bishops Court, Cape Town, South Africa and maintained as per *N. furzeri* [23]. Fish were fed twice per day for six days and fasted one day per week. A 50% water change was performed weekly. Water for the water changes was prepared before the time using 15 g iodated coarse salt, 2 g MgSO₄ and 2 g KHCO₃ per 20 L and then filtered over limestone to compensate for the soft municipal tap water and its unstable pH. Fish were maintained in accordance with ethical standards of animal care.

Buffers

All dry chemicals, unless otherwise noted, were obtained from Merck.

The protein extraction buffer (pH 7.2) was composed of 0.1 M TRIS, 1% Nonidet P-40 substitute (Sigma, 74385), 0.01% SDS, 1 µg/mL Aprotinin (Roche, 10236624001) and 0.1 µM PMSF (Sigma P7626) (from a 0.1M stock prepared in isopropanol). The buffer was chilled to 4°C before use.

Phosphate buffered saline (PBS) solution consisted of 140 mM NaCl, 2.7 mM KCl, 8.8 mM Na₂HPO₄ and 1.47 mM KH₂PO₄ (pH 7.4). For western blots 500 µL of Tween (Sigma P1379) was added per L to produce the PBS-T. A TRIS buffered saline buffer (TBS) was employed for microglial staining with isolectin: 50 mM TRIS, 150 mM NaCl, 20 mM MgCl and 10 mM CaCl₂ (pH 7.4) Blocking solution consisted of 1% BSA (Roche, 735078) in PBS or TBS. A 5% milk solution in PBS was used as blocking solution for western blots.

SDS-PAGE gels were prepared as per Current Protocols [24].

Tank buffer for SDS-PAGE was made up of 3 g TRIS together with 14.4 g glycine and 10 mL 10% SDS to 1 L with mQH₂O. Transfer buffer

was composed of 44 mM TRIS, 182 mM glycine and 200 mL methanol diluted to 1 L with mQH₂O. 5× loading dye was prepared from 4 mL 10% SDS mixed together with 2 mL 100% glycerol, 1 mL β-mercaptoethanol, 2.5 mL 0.5 M TRIS (pH 6.8) and 0.003 g bromophenol blue and made up to 10 mL with mQH₂O.

Anti-fade mowiol mounting medium was prepared by adding 2.4 g mowiol (Farbwerker Hoescht, Frankfurt Germany) to 6 mL glycerol, left to stir until completely dissolved whereafter 6 mL mQH₂O was added. To this, 12 mL 0.2 M TRIS (pH 8.5) was added. The solution was incubated for 1 hour at 50°C and then centrifuged at 12000×g for five minutes. The supernatant was collected and stored at -20°C. For use, an aliquot was thawed to room temperature and n-propyl gallate (Sigma, P3130) was added, the aliquot vigorously shaken, left to stand overnight at 4°C and then centrifuged at 12000×g for five minutes. The anti-fade mowiol was stored at 4°C.

Dissection and preparation of tissue samples: Fish were sacrificed and the tissue dissected in cold PBS as discussed in [3]. The lenses were removed following which the cranial bones were pried apart and the brain (with eyes attached) placed into 4°C PBS and then into tissue freezing medium (Jung, 020108926) and left to stand on ice for 30 minutes to dehydrate the brain prior to freezing at -80°C.

For protein extraction, the eyes were severed from the optic nerve and the spinal cord severed from the brain below the cranial nerves and then placed into an eppendorf test tube containing 200 µL protein extraction buffer. The tissue was homogenized and then centrifuged and the debris discarded. Protein samples were aliquoted and stored at -80°C.

Histochemical staining: For wax mounting and sectioning whole fish were fixed in Bouins solution [25] and sectioned at 5 µm. Sections were stained with Kluver & Barrera Luxol Fast Blue/Cresyl Violet. All techniques, fixatives and stains prepared as in Bancroft & Gamble [26].

Immunohistochemistry of brain sections: Frozen brains with attached eyes were sectioned at 20 µm (for confocal analysis) at -20°C in a cryostat and sections fixed to APTES coated slides.

Sections were permeabilized in -20°C methanol for 10 minutes and

Antibody	Immunohistochemistry		Western blots	
	dilution	reactivity	dilution	reactivity
E578 anti-L1 [†]	1 : 2000	yes	1 : 2000	yes
GA-5 mab antiGFAP (Sigma G6171)	1 : 2000	yes	1 : 2000	yes
rabbit anti-bovine GFAP (DAKO Z0334)	1 : 2000	yes	1 : 2000	yes
SMI31(Covance SMI-31R)	1 : 400	yes	1 : 1000	yes
mab anti-rat TNR [‡]	1 : 400	yes	1 : 400	yes
rabbit anti-mouse S100 (Sigma S2644)	1 : 1000	inconsistent	1 : 1000	no
anti-Integrin β1 (Sigma SAB4501582)	1 : 200	no	N/A	N/A
rat anti-mouse MBP [§]	1 : 20	no	N/A	N/A
anti-zebrafish TAG [¶]	1 : 200	no	N/A	N/A
anti-mouse β-tubulin (Covance PRB-435P)	1 : 1000	no	N/A	N/A

[†]Gift from C. Stuermer, Konstanz Germany.

[‡]Gift from P. Persheva, Bonn Germany.

[§]Gift from C. Linington, Munich Germany.

[¶]Product from Lang et al. [10].

Table 1: Antibodies used in this study along with dilutions and reactivity results. Antibodies which were not reactive on IHC sections were not tested against western blots.

then given three washes in PBS. Sections were then incubated for one hour in blocking solution and then overnight at 4°C in blocking solution with primary antibodies. Antibody dilutions are summarized in Table 1. After incubation with primaries, the sections were washed three times in PBS and then incubated for 90 minutes at room temperature in the dark with anti-rabbit Alexa 488 (Molecular Probes, Invitrogen) and anti-mouse Cy3 (Jackson Immuno Research) (each diluted 1:1500). After secondary incubation, sections were washed in PBS and then mounted in anti-fade mowiol.

For biotinylated lectin staining, endogenous biotin was blocked for one hour at room temperature with DAKO Vector-Stain kit avidin-DH (Vectastain, PIC6100) added to TBS with 1% BSA according to the manufacturers specifications whereafter the slides were rinsed in TBS and incubated in 0.1 mg/mL biotin (Sigma, B4501) for 15 minutes and then washed in TBS. After washing, the BS-I isolectin B4 (Sigma, L3140) was incubated overnight on the sections at 1:60 dilution of 1 mg/mL isolectin solution into a TBS blocking solution of 0.1 mg/mL biotin and 1% BSA. After incubation, the sections were washed and incubated under streptavidin-Alexa 488 (Sigma) diluted 1:500 in TBS blocking solution for 90 minutes; and then washed and incubated under 0.5 µg/mL DAPI for 10 minutes before being washed and mounted in anti-fade mowiol.

SDS-PAGE and western blotting: Protein determinations of homogenates were done using the Pierce BCA protein assay (Pierce, 23225). Samples were read at 695 nm on a Kayto RT-2100C microplate reader.

Protein samples were incubated at 95°C in loading dye for two minutes. Samples which were to be incubated with E587, anti-TNR were incubated at 95°C in a loading dye without β-mercaptoethanol. For the E587, TNR and SMI31 blots, 20 µg protein was loaded onto a 7.5% SDS-PAGE gel (acrylamide, Sigma, A3574). For the GFAP blots, 5 µg protein was loaded onto 12% SDS-PAGE gels. pQGold IV protein marker (pQLab, 27-2116) was used. Electrophoresed protein was transferred to Amersham Hybond-ECL (General Electric) paper using transfer buffer at 100 V for one hour.

The blot was blocked for one hour in 5% commercial milk powder in PBS-T buffer whereafter the primary antibody was added together with 5% milk in PBS-T and incubated overnight at 4°C. Antibody dilutions are summarized in Table 1. The blot was washed four times in PBS-T and then the secondary antibodies were added: goat anti-rabbit-HRP (Biorad, 170-6515) and goat anti-mouse-HRP (Biorad, 170-6516) at 1:1500 dilution for 60 minutes. For autoradiograph visualization the blot was washed four times in PBS-T and then SuperSignal West Pico Chemiluminescent reagent (Pierce, 34080) was applied. Alternatively the blots were developed using a metal intensified DAB protocol based on Adams [27].

Sizes were calculated using a linear regression of a graph of molecular mass (kDa) vs the log of the migration distance (in millimeters) through the gel. The largest marker band was 170 kDa and the smallest 5 kDa.

Microscopy: Images were obtained using a Zeiss Confocal microscope (Jena, Germany). Images are representative of several specimens and were edited for publication using Adobe Photoshop CS2 v9.0.2.

Results and Discussion

Results of SMI31 and anti-GFAP labeling

Figure 1 shows a luxul fast blue/cresyl violet stain of an 5 µm optic

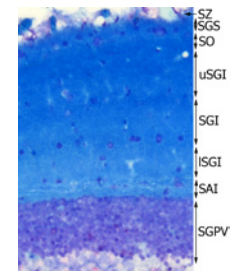


Figure 1: 5µm fixed section of optic tectum of *Nothobranchius guentheri* stained with Luxol Fast Blue and Cresyl Violet. Optic tectum layers are labeled on the Figure: SZ, stratum zonale; SGS, stratum griseum superficiale; SO, stratum opticum; uSGI, upper stratum griseum intermediale; SGI, stratum griseum intermediale; ISGI, lower stratum griseum intermediale; SAI, stratum album intermediale; and SGPV, stratum griseum periventriculare. Neuronal cell bodies appear purple and myelin light blue. 400× magnification.

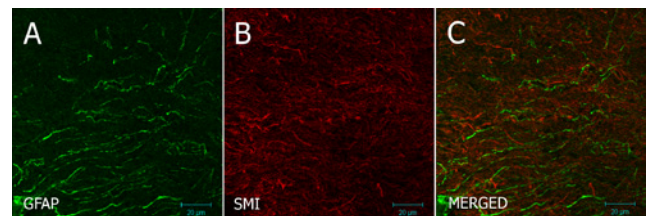


Figure 2: 20 µm frozen section of optic nerve of *Nothobranchius guentheri* probed with rabbit anti-cow GFAP and with SMI31 antibodies. The nerve is filled with axon fibers as well as large glial processes. Signals do not colocalize. Scale bar = 20 µm.

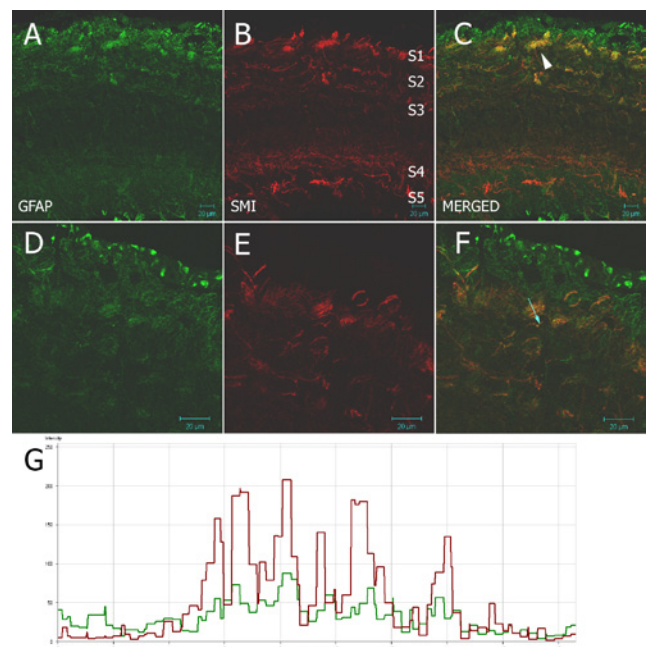


Figure 3: 20 µm frozen section of optic tectum of *Nothobranchius guentheri* probed with rabbit anti-cow GFAP and with SMI31 antibodies. There is a strong GFAP positive layer corresponding with the SZ into the SO (Figure 1) which is indicative of radial glia. The SMI31 signal is seen in five discrete zones: S1 the SGS & SO; S2 the uSGI; S3 the SGI; S4 the SAI; and S5 the SGPV. SMI31 and anti-GFAP signal are seen to overlap in cage-like structures in the SGS which are enlarged in Figures D-F. There is some co-localization of SMI31 and anti-GFAP signal (Figures F & G) in these structures. Scale bar = 20µm.

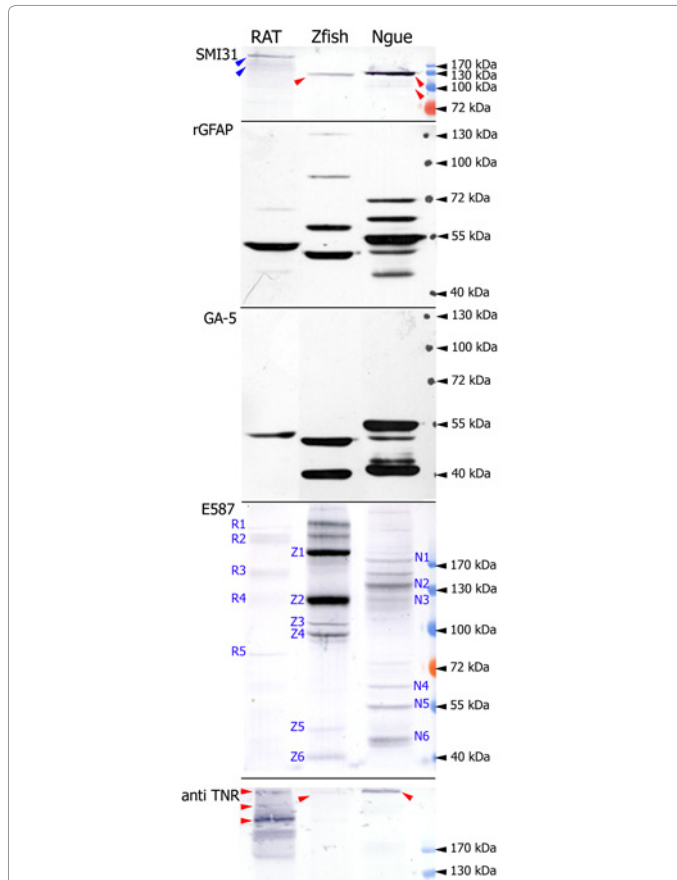


Figure 4: Western blots against brain homogenates of rat, zebrafish (Zfish) and *N. guentheri* (Ngue). The antibodies used are SMI31 which should label neurofilament protein of approximately 110 to 230 kDa for the rat. Rat bands are indicated by blue arrowheads and fish in red. Two GFAP antibodies were used, the rabbit polyclonal anti-cow GFAP (rGFAP) and the mouse monoclonal anti-human GFAP (GA-5) which should label proteins of approximately 50 kDa. The E587 antiserum is generated against goldfish L1 and should label proteins of 190, 120 and 70 kDa. Rat bands are labels R1–5, zebrafish Z1–6 and *N. guentheri* N1–6. The monoclonal anti-TNR antibody labels three bands in the rat lane (blue arrowheads) and one band each in the fish lanes (red arrowheads). Marker band sizes are indicated to the right of the blots.

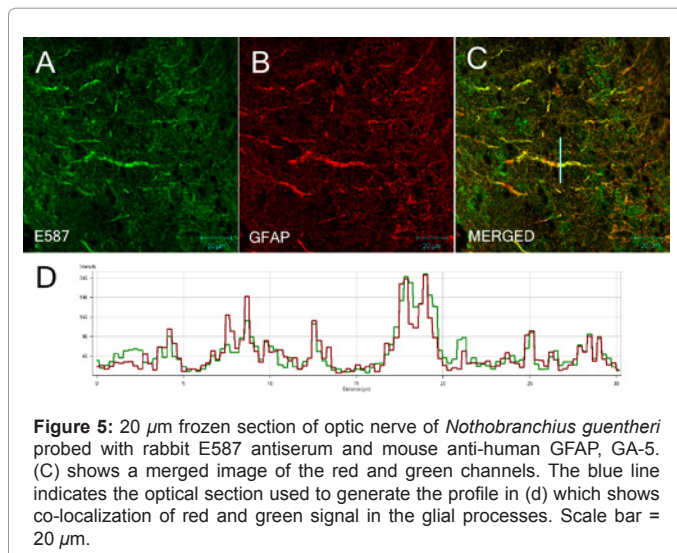


Figure 5: 20 μm frozen section of optic nerve of *Nothobranchius guentheri* probed with rabbit E587 antiserum and mouse anti-human GFAP, GA-5. (C) shows a merged image of the red and green channels. The blue line indicates the optical section used to generate the profile in (d) which shows co-localization of red and green signal in the glial processes. Scale bar = 20 μm .

tectum (OT) section of *N. guentheri* and serves as reference for the below text.

It is expected that the SMI31 and rabbit anti-GFAP antibodies would label nerve fibers and astroglial-like structures (radial glia in particular as is typical for fish) respectively.

Figure 2 shows a section through the optic nerve (ON). The nerve is filled with SMI31 immunoreactive nerve fibers as well as large anti-GFAP immunoreactive glial processes. Signals do not colocalize. Figure 3 A–G show a strong anti-GFAP immunoreactive layer corresponding with the stratum zonale (SZ, see Figure 1 in reference to OT layers) which is lined with radial glial cell bodies. This layer stretches into the stratum opticum (SO). There is also strong anti-GFAP reactivity in the stratum griseum periventriculare (SGPV) as would be expected for radial glia. The SMI31 signal is seen in five discrete zones: S1 the stratum griseum superficiale (SGS) and SO; S2 the upper stratum griseum intermediale (uSGI); S3 the stratum griseum intermediale (SGI); S4 the stratum album intermediale (SAI); and S5 the SGPV which are composed mostly of axon fibers and dendritic projections as shown for goldfish [28]. SMI31 and anti-GFAP signal colocalize in cage-like structures in the SGS which are enlarged in Figures 3 D–G. SMI31 signal was observed in both one week old fry (data not shown) and aged fish. In *Nothobranchius* species the epitope targeted by SMI31 may be present on neurofilament regardless of age and degenerative state as has been demonstrated by Lee et al. [29] in rats.

The SMI31 western blot (Figure 4) showed bands in the rat lane of approximately 226 and 155 kDa which corresponds with the predicted masses of the phosphorylated heavy and medium isoforms [5,30]. This antibody produces a single band of ≈ 120 kDa in the zebrafish lane. Two bands are visible in the *N. guentheri* lane. These are approximately 114 and 134 kDa. With extended development a third band of ≈ 123 kDa became visible, which ultimately developed into a smear from 114 to 134 kDa. This multiple banding is typical of phosphorylated neurofilaments [6]. The size of the *N. guentheri* SMI31 immunoreactive bands and those of the mammalian medium chains, which range from 110 to 145 kDa, are coincidental. The lamprey neurofilament proteins range from 180 kDa to 50 kDa, with one neurofilament being 132 kDa [31]. The SMI31 antibody merely recognizes the same evolutionary conserved tyrosine-phosphorylation motif common to phosphorylated neurofilaments [32]. No smaller SMI31 reactive bands were observed.

The rabbit anti-cow GFAP antibody reacted with the homogenates to reveal several bands in each lane (rGFAP, Figure 4). Two bands were detected in the rat lane, the major band being ≈ 52 kDa, the other close to 70 kDa, possibly corresponding with neurofilament L which polyclonal GFAP antibodies are known to cross-react with [33]. A 50 kDa band is detected in the zebrafish lane with additional larger bands. Five bands are visible in the *N. guentheri* lane: the major band is ≈ 55 kDa (and appears to be a smear of two very similar sized bands), the two smaller bands are 45 and 51 kDa. One of the larger bands is ≈ 61 kDa and the other ≈ 69 kDa.

The polyclonal GFAP antibody used by the authors, Z0334 from DAKO, was used by Korolainen et al. [34] against aged and demented brain samples and also yielded a multiple banding pattern with a major band at 50 kDa and several smaller bands down to 35 kDa. The bands were confirmed to be GFAP and its post translational products by means of HPLC-ESI-MS/MS. This multiple banding pattern was observed for rainbow trout brain homogenates where a polyclonal anti-goldfish GFAP antibody was used [35]. However, trout astroglia grown in culture only produced a prominent band at 51 kDa suggesting that in

fish, as in mammals, there is significant post-translational modification (as well as oxidation and degradation) of GFAP in the intact CNS in addition to multiple isoforms being expressed. It is known that the GFAP ϵ isoform is post-translationally modified by presenilin proteins [36]. The multiple banding pattern observed on the blots shown in Figure 4 is the expected outcome of using GFAP antibodies against brain homogenates. To obtain a solitary \approx 50 kDa band would be extraordinary against a brain homogenate.

The neurofilament tyrosine-phosphorylation motif is common to GFAP and nuclear lamin [32] but SMI31 does not cross-react with other proteins on the blots. However, the polyclonal anti-GFAP does cross-react with proteins of approximately 61, 69 and 114 kDa as predicted from [32,37]. Middeldorp et al. [33] observed GFAP expression in degenerating neurons in culture using the Z0334 polyclonal GFAP antibody. This antibody was reacting against neurofilament L, a \approx 68 kDa protein in humans. They hypothesize that the inclusion of neurofilament L into NFTs renders it susceptible to recognition by GFAP antibodies. On western blots using the GA-5 and Z0334 antibodies bands of 61 and 69 kDa are detected and the neurofilament L gene which has been cloned from the lamprey [31] is shown to share 44% amino acid sequence homology with the human neurofilament L and have an apparent molecular mass of 64 kDa. Nuclear lamins are \approx 70 kDa but as the structures in Figure 3F occur outside of the nucleus it is unlikely to be cross reactivity with lamins but with the neurofilament L. An alternative explanation is that of ghost tangles. These are extracellular NFTs which are insoluble debris from degenerate neurons and have also been observed to be GFAP positive remains of astrocytic processes into the NFTs [38]. These ghost tangles do take on a cage-like appearance in sections.

As the SMI31 antibody did not cross react with neurofilament L on the blot the structures where SMI31 and polyclonal GFAP colocalize must also include the 114–132 kDa neurofilament proteins. Whether the GFAP signal in Figure 3F is the product of Z0334 reactivity against neurofilament L in NFTs or GFAP in ghost tangles remains to be determined. Research is underway to determine if the frequency of these cage-like structures can be correlated with age and the incidence and location of tangles and plaques in the OT of *N. guentheri*.

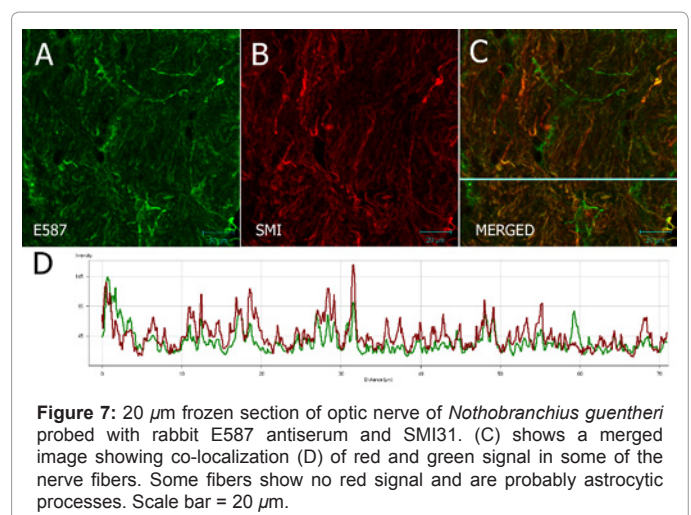
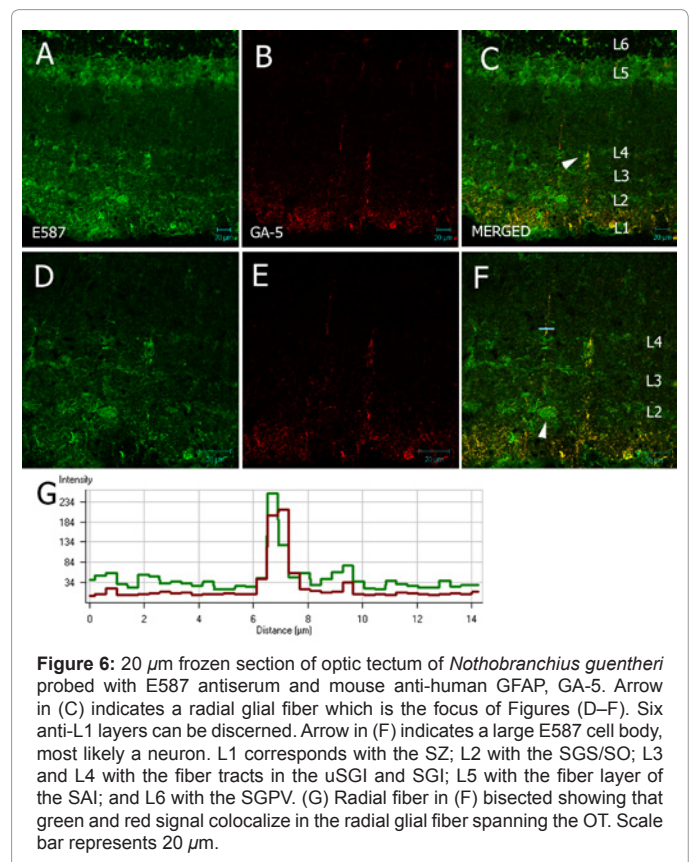
Results of GA-5 anti-GFAP and E587 labeling: We expect the E587 antiserum to label astroglia in the ON and OT as well as to label neurons and nerve fibers independently of the GA-5 monoclonal anti-GFAP antibody.

Figure 5 shows strong colocalization between E587 and GA-5 antibodies and the structures are consistent with those of astrocytic projections through the ON. In Figure 6 there is colocalization between E587 and GA-5 antibodies, both in the SZ and in radial glial-like structures which span the OT. The E587 signal is distributed through six distinct layers (Figure 6D): the SZ, SO, uSGI, SGI, SAI and SGPV. These results are consistent with the expected pattern of L1 distribution through the OT. Some large E587 cell bodies are visible in the OT (arrow head, Figure 6F).

The anti-human GFAP antibody, clone GA-5, reveals one band at \approx 52 kDa for the rat brain homogenate (Figure 4). Zebrafish brain homogenate reacts with GA-5 to reveal two major proteins of approximately 43 kDa and 50 kDa in size. For *N. guentheri* there are five bands: a major band at \approx 55 kDa paired with a smaller one of about 51 kDa; and another major band at \approx 43 kDa together with two less prominent larger bands of approximately 45 and 48 kDa. The GA-5 clone is known to give the observed banding pattern, as can be seen for

the Santa Cruz GA-5 antibody (sc-58766) [39], but still reliably labels astroglia only [32,40]. Similarly, the J1-31 clone also gives a multiple banding pattern against whole brain homogenates but also reliably labels only astrocytes [37]. García et al. [37] attribute this multiple banding pattern to phosphorylation and degradation of GFAP. With longer exposure other bands manifested in all lanes when using both the rabbit anti-GFAP and GA-5 antibodies (data not shown). For all species, using the GFAP antibodies, bands appear between the 100 and 130 kDa. These could be the product of cross-reactivity between GFAP antibodies and neurofilaments.

The human L1 is 220 kDa and is cleaved at multiple sites by several



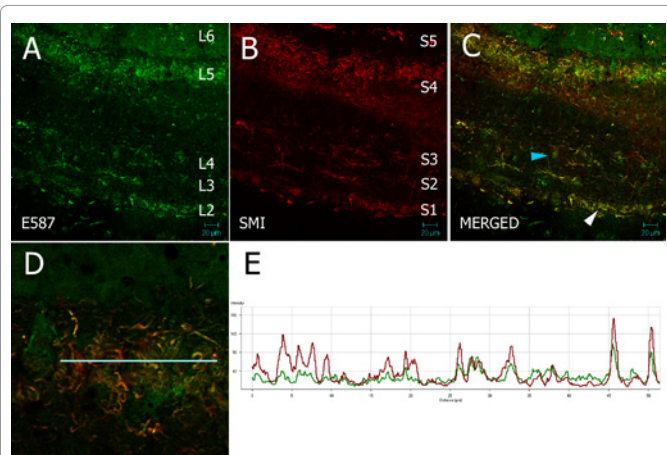


Figure 8: 20 μm frozen section of optic tectum of *Nothobranchius guentheri* probed with rabbit E587 antiserum and mouse SMI31. Several discrete SMI31 and E587 layers are evident in (A) and (B) which partially overlap in the merged image (C). Blue arrow in (C) indicates a large E587 cell body, possibly a neuron. White arrow in (C) serves as the centre of focus for (D). Red and green signal in (D) colocalize (frame E) and show a complex of SMI31 and E587 positive fibers in the SGS/SO layer.

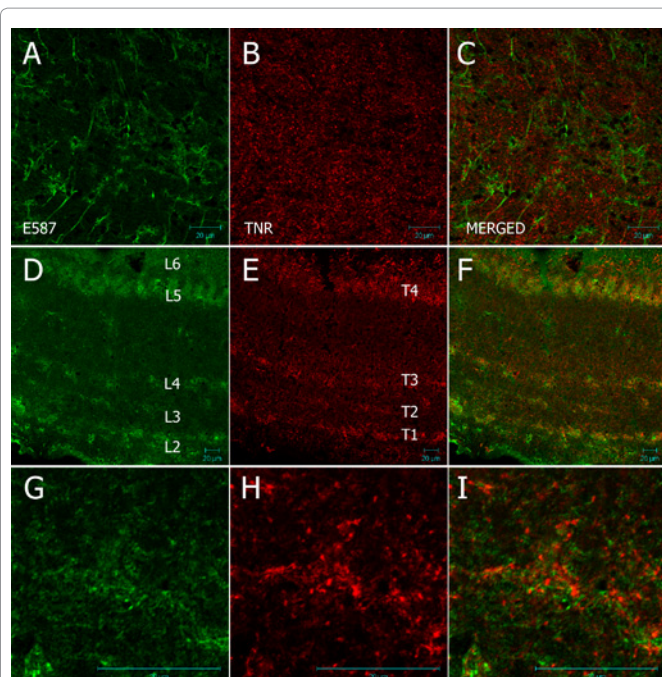


Figure 9: 20 μm frozen section of optic nerve and optic tectum of *Nothobranchius guentheri* probed with rabbit E587 antibody mouse anti-TNR. (A–C) shows images of the ON. E587 positive astrocytic processes are visible along with anti-TNR signal which appears restricted to specific cell bodies. There is no evidence for colocalization as in Figures 5 and 7. (D–F) shows images of the OT. The anti-TNR signal (E) is ordered in four layers corresponding with the SO (T1); uSGI (T2); SGI (T3); and SAI (T4) into the SGPV. These layers appear broader than the corresponding E587 layers and each layer fades in the direction of the inner layers of the tectum. (G–I) show magnified images of the OT which clearly show that E587 and anti-TNR signal do not colocalize. The anti-TNR signal is restricted to small cell bodies in the tissue. Scale bar = 20 μm .

and 17 as well as γ -secretase results in a 28–32 kDa membrane bound fragment and a \approx 200 kDa soluble fragment [42]. The concentration of the large soluble fragments in patients with dementia have been observed to increase compared to age-matched controls [12]. This array of post-translational modifications could generate an eight band pattern on a blot using a polyclonal serum. The multiple banding patterns shown in Figure 4 is expected for a protein which undergoes such extensive post-translational modification in addition to glycosylation.

The E587 antiserum detected bands of approximately 269, 238, 157, 125 and 85 kDa in the rat lane (bands R1–R5). Based on the human pattern a \approx 30 kDa was expected but could not be resolved on the 7.5% gel. The band sizes which do arise are within the expected range for mammalian L1 [12,41,42] based on the errors associated with bands larger than 170 kDa. Bands of 190, 120 and 70 kDa are expected for E578 against zebrafish [43]. The authors, using a metal intensified DAB developed blot, demonstrate bands of 199, 125 and 97 kDa (Z1, 2 & 4 respectively, Figure 4) in addition to several other bands. The observed differences to Weiland et al. [43] could be due to differences in the origin of our zebrafish (an outbred aquarium strain) or the limits of the chemiluminescent method employed by Weiland et al. [43] which is prone to over-develop some bands at the expense of other bands. Z4, 5 & 6, of molecular masses 97, 52 and 42 kDa sum to 199 kDa which is the same the size obtained for Z1. Similarly the three smallest visible bands in the *N. guentheri* lane, N4, 5 & 6 (68, 60 & 48 kDa), sum to 176 kDa which is the same size as N1. The E587 antibody is producing a similar banding pattern against the rat, zebrafish and *N. guentheri* brain samples. The observed differences between the banding patterns among the fish may represent differences in post-translational modification of the full length protein as well a differences in total length. E587 is probably reacting against a structurally similar protein in each sample.

Results of SMI31 and E587 labeling: SMI31 and E587 signal is expected to colocalize in dendrites and in some axons fibers. E587 is also expected to label neurons. Figure 7 shows SMI31 signal in axon fibers in the ON as per Figure 2. Fibers are predominantly SMI31 positive but there is also strong E587 signal in some axons. E587 signal is also present in the astroglial projections in the ON as seen in Figure 5. The colocalization between SMI31 and E587 immunoreactivity in Figure 7 could be due to up-regulation during axon extension and then down-regulation once the connection with the target neuron is established in accordance with its role in axon guidance [10,44,45].

Figure 8 shows five SMI31 positive layers in the OT as well as five of the six E587 layers seen in Figure 6. Layers L2–L6 and S1–S5 overlap (Figure 8d) and correspond with the SGS/SO, uSGI, SGI, SAI and SGPV. A complex of SMI31 and E587 positive fibers in the SGS/SO where fibers from the ON are expected to synapse with neurons in the SGS are visible in Figure 8E. The neurons of the SGS synapse with neurons in the uSGI and SGI. These fibers are strongly positive for both SMI31 and E587. These neurons synapse with neurons in the uSGI and SGI. These fibers are strongly positive for both SMI31 and E587 and are most likely dendrites expressing L1 in regard to L1's role in plasticity. In addition, the E587 antiserum also labels large cell bodies in the OT.

Results of anti-TNR and E587 labeling: Figure 9A–C shows anti-TNR signal restricted to the myelin layers of the ON, with no colocalization with the E587 signal which labels astroglia and nerve fibers. Figure 9D–F show the anti-TNR signal ordered over four layers corresponding with the SO (T1); uSGI (T2); SGI (T3); and SAI (T4) into the SGPV. These layers appear broader than the corresponding E587 layers and each layer fades in the direction of inner layers of

different enzymes [12,41]. The 220 kDa protein is cleaved into a membrane bound C-terminal fragment of 80 kDa and a soluble 140 (by plasmin) or 180 kDa fragment (by neuropsin). Cleavage by ADAM10

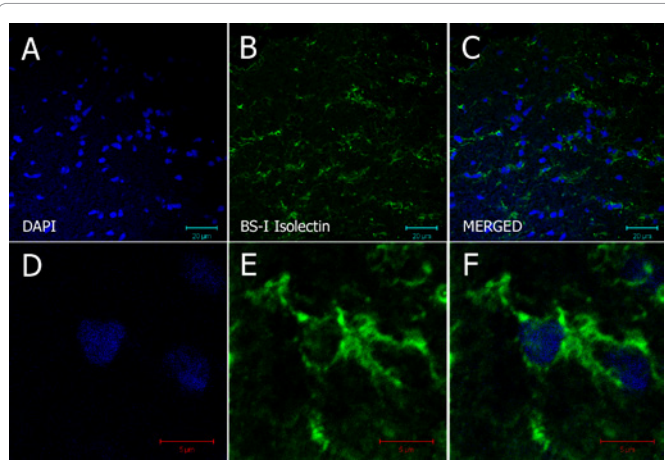


Figure 10: 20 μm frozen section of optic nerve of *Nothobranchius guentheri* probed with DAPI and biotinylated BS-I Isolectin B4. (A–C) shows images of the ON containing microglia labeled with GS-isolectin. Typical microglial morphology can be observed in the enlarged frames (D–F). Scale bars = 20 μm for (A–C) and 5 μm for (D–F).

the OT. Figure 9G–I shows that anti-TNR signal is localized to small cellular bodies. This punctate pattern of anti-TNR staining is unlike that of astroglial, neuronal or axonal labeling by the other antibodies. As expected, the anti-TNR antibody labels the myelinated nerve fiber tracts in the OT.

E587 labeled oligodendrocytes in the goldfish [45] though it did not colocalize with TNR in *N. guentheri*. It may be that *N. guentheri* oligodendrocytes either do not express L1 at all or do not express an L1 recognizable by E587. It has been reported that glia and neurons express different forms of L1 [46].

The anti-TNR antibody produced three bands for the rat but only one for *N. guentheri* and zebrafish (Figure 4). These proteins are glycosylated in situ and as such the determinations of molecular masses by western blot are unreliable. Also, all prominent bands (except one of the rat bands) fall outside of the marker band range. Mammalian TNR has a molecular size of 160–180 kDa and can form dimers and trimers [47,48]. Only the ≈ 165 kDa band falls within the marker range of the western blot and is of the expected size. The TNR antibody does not cross react with smaller proteins on the blot indicating high specificity. The fish anti-TNR reactive proteins did not migrate into the resolving gel and appears to be of similar size to the band at the top of the rat lane. No cross-reactivity with other proteins was observed in the *Nothobranchius* lane. The western blot data together with the IHC data provides no evidence to suppose that the TNR antibody is not labeling TNR in *N. guentheri* tissues.

Results of labeling with GS-I Isolectin B4: Figure 10A–C is of the ON containing microglia labeled with isolectin and DAPI. Figure 10D–F are enlargements of the microglia indicated in A–C. These show the typical microglial form. Unexpectedly, the same sections used to observe microglia in the ON showed no microglia in the OT (data not shown). Within the OT the BS-I isolectin did bind to the cell walls of blood vessels confirming that the lectin was present over that part of the tissue section during the incubation step. The absence of BS-I isolectin positive microglia in the OT was unexpected. However, the possibility exists that there are microglia present in the OT but that they are not labeled by BS-I isolectin.

There is no evidence thus far that TNR is repulsive of *Nothobranchius* microglia.

Other antibodies tested: Five other antibodies were tested on *N. guentheri* sections but found to be inactive or inconsistent (results not shown). These are summarized in Table 1. The inactivity of the MBP antibody was surprising as it has been effective against goldfish, *Xenopus*, *Gallotia galloti* and rodents in our laboratory. The β -tubulin antibody has also been ineffective against zebrafish. The ineffectiveness of the TAG and integrin antibodies suggest that these proteins may be too evolutionary diverse in nature to be generally useful. Strong s100B staining was obtained in one cohort of aged *N. guentheri* but was totally absent in other aged cohorts. The s100B antibody did not react with protein on western blots.

Conclusions

The *Nothobranchius* research community now has available to it antibodies against nerve fibers (SMI31), astroglia (anti-GFAP) and oligodendrocytes (anti-TNR) in addition to the E587 antiserum which labels young axons and radial glial fibers, and the BS-I Isolectin which labels ON and retinal microglia.

SMI31 was consistent with expectations of neurofilament distribution in neuronal tissues. Together with the data from the western blots we find no evidence to believe that the SMI31 is not targeting neurofilament protein in *N. guentheri* and is a reliable label of axons and dendrites.

Some uncertainty exists as to the fidelity of E587 and GFAP antibodies. The combination of IHC and western blot data indicate that the E587 antiserum is labeling an L1-like protein or proteins in *N. guentheri*. We cannot exclude that the E587 antiserum is not detecting other NCAMs in addition to L1 (such as CHL1, a 185 kDa protein in mammals), but if it is unreliable for detecting L1 in rat and *N. guentheri* brain homogenates then our blots reveal that it is equally unreliable for zebrafish as several additional bands developed on our blot compared to that published by Weiland et al. [43]. If the structures in Figure 3F prove to be neurodegenerative features then the reactivity of the polyclonal GFAP would be consistent with expectations based on the literature. Both GFAP antibodies reliably labeled astrocytes and did not label non-astrocytic structures.

Regardless of the uncertainties, all of the antibodies reliably label expected cell types and structures in the *Nothobranchius* nervous system which makes it possible to detect aging related changes at the cellular level in the *Nothobranchius* CNS. This research highlights the need to clone and express the respective proteins believed to be labeled by these antibodies and generate more specific antibodies against these proteins.

Experiments are underway to study neurodegeneration in *N. guentheri* using these antibodies as cellular markers as well as test them against other *Nothobranchius* species.

Acknowledgements

The authors wish to thank Mr. Otto Schmidt for supplying the fish. Also, Mrs T. Wiggins, S. Cooper, M. Petersen and Ms B. Kleemann for technical assistance. Funding was supplied by the author (TG), Mr Raymond Ackerman, Jean Huber (www.killi-data.org), the University of Cape Town and the South African National Research Foundation. We also wish to thank Mr. D.A. Wilcox for proof reading the manuscript and making valuable suggestions.

References

1. Genade T, Benedetti M, Terzibasi E, Roncaglia P, Valenzano DR, et al. (2005) Annual fishes of the genus *Nothobranchius* as a model system for aging research. *Aging Cell* 4: 223-233.

2. Terzibasi E, Valenzano DR, Benedetti M, Roncaglia P, Cattaneo A, et al. (2008) Large differences in aging phenotype between strains of the short-lived annual fish *Nothobranchius furzeri*. PLoS ONE 3: e3866.
3. Valenzano DR, Terzibasi E, Genade T, Cattaneo A, Domenici L, et al. (2006) Resveratrol prolongs lifespan and retards the onset of age-related markers in a short-lived vertebrate. Curr Biol 16: 296-300.
4. Valenzano DR, Terzibasi E, Cattaneo A, Domenici L, Cellerino A (2006) Temperature affects longevity and age-related locomotor and cognitive decay in the short-lived fish *Nothobranchius furzeri*. Aging Cell 5: 275-278.
5. Wang J, Tung Y, Wang Y, Li X, Iqbal K, et al. (2001) Hyperphosphorylation and accumulation of neurofilament proteins in Alzheimer Disease brain and in okadaic acid-treated SY5Y cells. FEBS Lett 507: 81-87.
6. Yang X, Yang Y, Luo Y, Li G, Yang E (2009) Hyperphosphorylation and accumulation of neurofilament proteins in transgenic mice with Alzheimer presenilin 1 mutation. Cell Mol Neurobiol 29: 497-501.
7. Nagele RG, Wegiel J, Venkataraman V, Imaki H, Wang KC, et al. (2004) Contribution of glial cells to the development of amyloid plaques in Alzheimer's Disease. Neurobiol Aging 25: 663-674.
8. Schmid R, Maness P (2008) L1 and NCAM adhesion molecules as signaling coreceptors in neuronal migration and process outgrowth. Curr Opin Neurobiol 18: 245-250.
9. Chen L, Zhou S (2010) "CRASH"ing with the worm: insights into L1CAM functions and mechanisms. Dev Dyn 239: 1490-1501.
10. Lang D, Warren JT Jr, Klisa C, Stuemmer CA (2001) Topographic restriction of TAG-1 expression in the developing retinotectal pathway and target dependent reexpression during axon regeneration. Mol Cell Neurosci 17: 398-414.
11. Becker T, Becker CG (2001) Regenerating descending axons preferentially reroute to the gray matter in the presence of a general macrophage/microglial reaction to a spinal transection in adult zebrafish. J Comp Neurol 433: 131-147.
12. Strekalova H, Buhmann C, Kleene R, Eggers C, Saffell J, et al. (2006) Elevated levels of neuronal recognition molecule L1 in the cerebrospinal fluid of patients with Alzheimer disease and other dementia syndromes. Neurobiol Aging 27: 1-9.
13. Lang D, Monson-Mayor M, Del Mar Romero-Aleman M, Yanes C, Santos E, et al. (2008) Tenascin-R and axon growth promoting molecules are up regulated in the regenerating visual pathway of the lizard (*Gallotia galloti*). Dev Neurobiol 68: 899-916.
14. Liao H, Bu WY, Wang TH, Ahmed S, Xiao ZC (2005) Tenascin-R plays a role in neuroprotection via its distinct domains that coordinate to modulate the microglia function. J Biol Chem 280: 8316-8323.
15. Kappler J, Baader S, Franken S, Pesheva P, Schilling K, et al. (2002) Tenascins are associated with lipid rafts isolated from mouse brain. Biochem Biophys Res Commun 294: 742-747.
16. Esposito G, Scuderi C, Lu J, Savani C, de Filippis D, et al. (2008) S100B induces tau protein hyperphosphorylation via Dickkopf-1 up-regulation and disrupts the Wnt pathway in human neuronal stem cells. J Cell Mol Med 12: 914-927.
17. He P, Shen Y (2009) Interruption of β -catenin signaling reduces neurogenesis in Alzheimer's disease. J Neurosci 29: 6545-6557.
18. Li HL, Wang HH, Liu SJ, Deng YQ, Zhang YJ, et al. (2007) Phosphorylation of tau antagonizes apoptosis by stabilizing β -catenin, a mechanism involved in Alzheimer's neurodegeneration. Proc Natl Acad Sci U S A 104: 3591-3596.
19. Salminen A, Huuskonen J, Ojala J, Kauppinen A, Kaamiranta K, et al. (2008) Activation of innate immunity system during aging: NF- κ B signaling is the molecular culprit of inflamm-aging. Ageing Res Rev 7: 83-105.
20. Bureau G, Longpré F, Martinoli MG (2008) Resveratrol and quercetin, two natural polyphenols, reduce apoptotic neuronal cell death induced by neuroinflammation. J Neurosci Res 86: 403-410.
21. Kim KY, Ju WK, Neufeld AH (2004) Neuronal susceptibility to damage: comparison of the retinas of young, old and old/caloric restricted rats before and after transient ischemia. Neurobiol Aging 25: 491-500.
22. Zhang F, Liu J, Shi JS (2010) Anti-inflammatory activities of resveratrol in the brain: role of resveratrol in microglial activation. Eur J Pharmacol 25: 1-7.
23. Genade T (2005) Laboratory manual for culturing *N. furzeri*. Nothobranchius information center.
24. Gallagher SR (1995) One-dimensional SDS gell electrophoresis of proteins. Curr Protoc Protein Sci 10: 1.1-1.34.
25. Woodhead AD, Pond V (1984) Aging changes in the optic tectum of the guppy *Poecilia (Lebistes) reticulatus*. Exp Gerontol 19: 305-311.
26. Bancroft JD, Gamble M (2007) Theory and practice of histological techniques. Churchill Livingstone 5th edn.
27. Adams JC (1981) Heavy metal intensification of DAB-based HRP reaction product. J Histochem Cytochem 29: 775.
28. Schmidt JT (1979) The laminar organization of optic nerves in the tectum of the goldfish. Proc R Soc Lond B Biol Sci 205: 287-306.
29. Lee VM, Carden MJ, Schaefer WW, Trojanowski JQ (1987) Monoclonal antibodies distinguish several differentially phosphorylated states of the two largest rat neurofilament subunits (NF-H and NF-M) and demonstrate their existence in the normal nervous system of adult rats. J Neurosci 7: 3474-3488.
30. Shea TB, Chan WK (2008) Regulation of neurofilament dynamics by phosphorylation. Eur J Neurosci 27: 1893-1901.
31. Jin LQ, Zhang G, Pennicooke B, Laramore C, Selzer ME (2010) Multiple neurofilament subunits are present in lamprey CNS. Brain Res 1370: 16-33.
32. Weigum SE, Garcia DM, Raabe TD, Christodoulides N, Koke JR (2003) Discrete nuclear structures in actively growing neuroblastoma cells are revealed by antibodies raised against phosphorylated neurofilament proteins. BMC Neurosci 4: 6.
33. Middeldorp J, van der Berge SA, Aronica E, Speijer D, Hol EM (2009) Specific human astrocyte subtype revealed by affinity purified GFAP antibody; unpurified serum cross-reacts with neurofilament L in Alzheimer. PLoS 4: e7663.
34. Korolainen MA, Auriola S, Nyman TA, Alanfuzoff I, Pirttilä T (2005) Proteomic analysis of glial fibrillary acidic protein in Alzheimer's disease and aging brain. Neurobiol Dis 20: 858-870.
35. Fröjdö EM, Westerlund J, Isomaa B (2002) Culturing and characterisation of astrocytes isolated from juvenile rainbow trout (*Oncorhynchus mykiss*). Comp Biochem Physiol A Mol Integr Physiol 133: 17-28.
36. Nielsen AL, Holm IE, Johansen M, Boven B, Jørgensen P, et al. (2002) A new splice variant of glial fibrillary acidic protein, GFAP ϵ , interacts with the presenilin proteins. J Biol Chem 277: 29983-29991.
37. Garcia DM, Weigum SE, Koke JR (2003) GFAP and nuclear lamins share an epitope recognized by monoclonal antibody J1-31. Brain Res 976: 9-21.
38. Ikeda K, Haga C, Oyanagi S, Iritani S, Kosaka K (1992) Ultrastructural and immunohistochemical study of degenerate neurite-bearing ghost tangles. J Neurol 239: 191-194.
39. Santa Cruz Biotechnology Inc (2011) GFAP (ga-5): sc-58766.
40. Franke FE, Schachenmayr W, Osborn M, Altmannberger M (1991) Unexpected immunoreactivities of intermediate filament antibodies in human brain and brain tumors. Am J Pathol 139: 67-79.
41. Schäfer MK, Altevogt P (2010) L1CAM malfunction in the nervous system and human carcinomas. Cell Mol Life Sci 67: 2425-2437.
42. Maretzky T, Schulte M, Ludwig A, Rose-John S, Blobel C, et al. (2005) L1 is sequentially processed by two differently activated metalloproteases and presenilin-1-secretase and regulates neural cell adhesion, cell migration, and neurite outgrowth. Mol Cell Biol 25: 9040-9053.
43. Weiland UM, Ott H, Bastmeyer M, Schaden H, Giordano S, et al. (1997) Expression of L1-related cell adhesion molecule on developing CNS fibre tracts in zebrafish and its functional contribution to axon fasciculation. Mol Cell Neurosci 9: 77-89.
44. Maness PF, Schachner M (2007) Neural recognition molecules of the immunoglobulin superfamily: signalling transducers of axon guidance and neuronal migration. Nat Neurosci 10: 19-26.
45. Ankerhold R, Leppert CA, Bastmeyer M, Stuermer CA (1998) E587 antigen is upregulated by goldfish oligodendrocytes after optic nerve lesion and supports retinal axon regeneration. Glia 23: 257-270.
46. Takeda Y, Asou H, Murakami Y, Miura M, Kobayashi M, et al. (1996) A nonneuronal isoform of cell adhesion molecule L1: tissue-specific expression and functional analysis. J Neurochem 66: 2338-2349.

47. Joester A, Faissner A (2001) The structure and function of tenascins in the nervous system. *Matrix Biol* 20: 13-22.
48. Hsia HC, Schwarzbauer JE (2005) Meet the tenascins: Multifunctional and mysterious. *J Biol Chem* 280: 26641-26644.